Dispersion-compensated microring photon pair source design with configurable purity–pair rate–heralding efficiency tradeoff

Kenneth M. Jabon[1,†], **Imbert Wang**[1] **and Miloš A. Popović**[1,‡]

[1]*Department of Electrical and Computer Engineering, Photonics Center, Boston University, Boston, MA 02215, USA*

[†]*kjabon@bu.edu,* [‡]*mpopovic@bu.edu*

Abstract: We present a Si microring-based photon pair source design with tailored pump/signal/idler escape rates allowing configurable purity-rate-heralding tradeoffs, while maintaining efficiency through tunable dispersion compensation. We validate the subcomponents using stimulated FWM experiments.

Several physical realizations of quantum computers employ networks of linear optical elements on a silicon photonics platform [1]. A source of high purity (γ) single photons is needed, to provide the quantum states that are acted on by linear optic quantum gates. In a quantum computing system, an array of photon pair sources may be used to entangle many photons concurrently, requiring a high generation rate of photon pairs in each device ($I_{src,pairs}$) and high escape (heralding) efficiency (η_{escape}) of those pairs. One cannot maximize all goal parameters simultaneously: there is an inverse relationship between $I_{src,pairs}$ and γ in photon pair sources [2]. Additionally, increasing η_{escape} (the ratio of photons coupling to the waveguide to photons generated) beyond a certain value decreases $I_{src,pairs}$. Because of these tradeoffs, a photonic system designer must target different operating regimes depending on their needs. A single photon source which can target different operating regimes – at "run-time" not design time – while maintaining a high generation rate would be a valuable component for enabling photonic quantum computing and other quantum information systems.

In this work, we propose a silicon microring resonator-based photon pair source that addresses these requirements, seen in Fig 1(a). The device has three components: a main photon pair generating ring, an auxiliary ring, and an interferometric coupler to the main ring. The main ring generates photon pairs via spontaneous four-wave mixing (FWM) from two input pump photons. The auxiliary ring corrects dispersion between resonances in the main ring, maximizing FWM efficiency (η_{FWM}). The interferometric coupler allows distinct, controllable coupling coefficients for the three ring resonances. We demonstrate the two sub-components of the device as separate structures as first steps towards demonstration of a pair-source including both. First, we demonstrate a tunable auxiliary ring correcting the dispersion of the main ring, improving η_{FWM} by satisfying the phase matching condition, thus increasing $I_{src,pairs}$ for any given device. Second, we demonstrate a two-point interferometric coupler, which sets the power coupling coefficients for each main ring resonance independently. These coefficients determine the critical properties of the device: $I_{src,pairs}$, η_{escape}, and γ of generated photons.

Before adding these sub-components, we maximize the FWM effiupciency [3]: $\eta_{fwm} \propto Q_{i,o}Q_{s,o}Q_{p,o}^2/V_{eff}^2$ where V_{eff} is the effective mode volume in the ring, with the Q_o including loss due to scattering, bending, and coupling (s: signal, p: pump, i: idler). We use this proportionality as a figure of merit to optimize the main ring geometry, resulting in a radius of 7.760 μm and a waveguide width of 0.460 μm for pair generation centered at 1550 nm.

Taking energy conservation in FWM ($E = hf$, and $2E_{pump} = E_{idler} + E_{signal}$) together with phase matching in the ring [3], we see η_{fwm} is maximized when the frequency spacing between modes is equal. Modal and material dispersion will generally cause an unequal spacing, or a finite $\Delta f_{FSR} = (f_i - f_p) - (f_p - f_s)$, which can be corrected for by introducing degenerate mode splitting at either the idler or signal frequency with a second ring [3]. In Fig. 1(b), we see an SEM image of the structure fabricated to isolate and test this effect. The aux ring radius of 5.281 μm allows only a single main-aux resonance overlap at a time with minimal crosstalk.

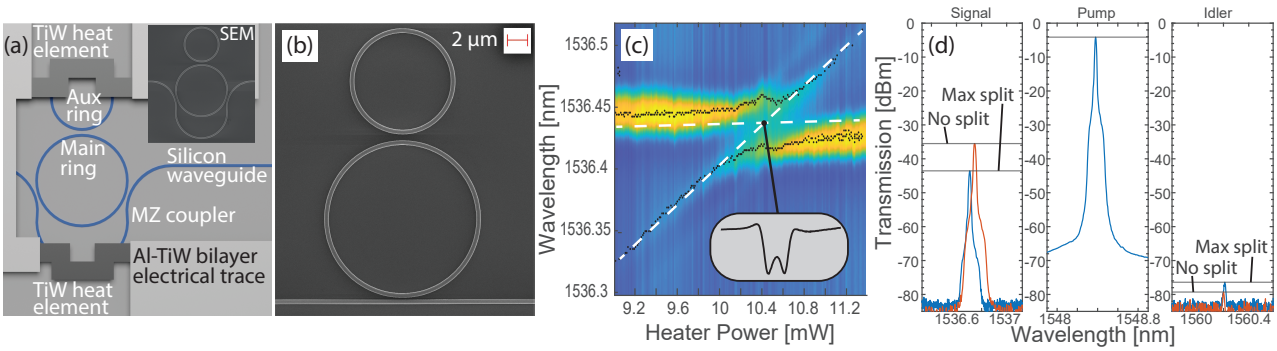

Fig. 1: Full photon pair source concept, and auxiliary (aux) ring characterization. (a) Rendering of full device concept. Center cavity (main ring), an aux ring for dispersion compensation, and a two-point coupler (MZ coupler) are collectively designed for maximum photon pair generation rate. Heaters are included for thermal correction of fabrication error. (b) SEM image of straight bus single point-coupled main ring, with aux ring, used to characterize and demonstrate dispersion compensation. (c) Measured wavelength positions of the aux (diagonal trace) and main ring (horizontal trace) resonances, as a function of heater power. Brighter colors indicate higher extinction ratio, black points indicate the resonance nadir. (d) Measured spectra of FWM of the structure with no mode splitting in orange, and at the optimum mode splitting which corrects for Δf_{FSR} in blue. The improvement in η_{FWM} is reflected by a gain in the idler peak relative to the uncorrected value by 2.87dB. Identical input pump and signal powers were used in all cases.

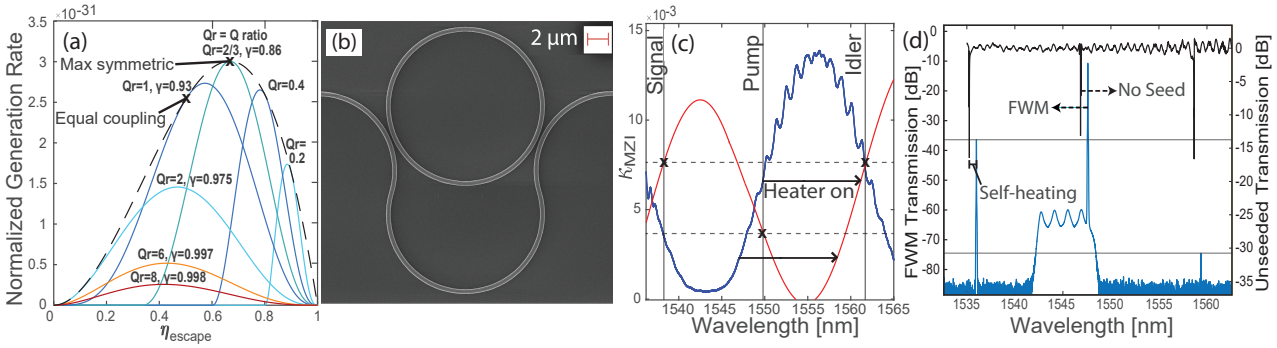

Fig. 2: Pair-source property tradeoffs of a symmetrically coupled ring ($r_{s,e} = r_{i,e}$), and characterization of interferometric coupler. (a) Normalized photon pair generation rate vs. photon escape efficiency, with each curve representing a different "Q ratio" ($Q_{s,i}/Q_p$); increasing Q-ratio increases purity γ. The MZ coupler can address any point by setting the coupling coefficients. The dashed line represents the maximum generation rate for a given η_{escape}, i.e. for a critically coupled pump. The device design addresses the point of maximum generation rate; greater than a device constrained to equal coupling. (b) SEM image of a subdevice fabricated to characterize the MZ coupler behavior. (c) The measured response (blue) of the MZ coupler when coupled to a waveguide rather than a ring. The Mach-Zehnder response gives specific power coupling coefficients at each resonance wavelength (vertical lines), which set the Q ratio. The device is offset to a smaller ΔL between arms, then heated to the designed response (red). (d) Bottom: Stimulated FWM in the device after MZ arm is heated to symmetric coupling condition. Top: measured spectra with same heating; no seed lasers.

We sweep the resonance wavelength of the auxiliary ring with the integrated heater, as shown by the diagonal line in Fig. 1(c), thus inducing mode splitting when the two rings' resonances intersect. The Δf_{FSR} for the main ring was simulated (measured) to be 2.58GHz (2.94 GHz), and a ring-ring gap of 550 nm was chosen to induce a splitting of double this at 5.16 GHz (5.08 GHz), reducing Δf_{FSR} to 0.4 GHz. As seen in a stimulated FWM measurement in Fig 1(d), the peak idler power (blue) nearly doubles (+2.9 dB), via an increased η_{fwm} by correcting for dispersion [3]. We also see a decrease in the transmitted signal power due to improved alignment with this resonance after performing this Δf_{FSR} correction and input wavelength optimization. A future iteration with a reduced ring-ring gap to adjust for the increase in measured Δf_{FSR} vs. simulation will completely eliminate the Δf_{FSR} for an even greater increase in η_{fwm}.

Symmetric coupling to the ring (i.e. external loss rate $r_{s,e} = r_{i,e}$, and intrinsic loss rate $r_{p,o} = r_{i,o} = r_{s,o} = r_o$; simulated: $3.13x10^9$ rad/s), achieves any combination of two of $I_{src,pairs}$, η_{escape}, or γ, the third being constrained by the others chosen at design time. It has also previously been shown to have greater $I_{src,pairs}$ than the equal coupling case at $\eta_{escape} > 0.5$ for a critically coupled pump [5]. Fig. 2(a) shows the normalized photon pair generation rate for a symmetrically-coupled ring, defined as [5]:

$$Normalized\ generation\ rate = \frac{I_{src,pairs,sym}}{(2\omega\beta_{fwm}P_p)^2} = \frac{r_{s,e}^2}{(r_{s,e}+r_o)^3}\frac{r_{p,e}^2}{(r_{p,e}+r_o)^4} \quad (1)$$

where $\eta_{esc} = \frac{r_{s,e}}{r_{s,e}+r_{s,o}}$. β_{fwm} is inversely proportional to V_{eff} and contains the nonlinear susceptibility of the material. P_p is the pump power input to the devuce, and ω is the frequency of operation. One can maximize $I_{src,pairs,sym}$ by traversing η_{esc} to the peak of each curve, or instead choose to maximize the η_{esc}, reducing $I_{src,pairs,sym}$. Several cases of "Q ratios" ($min(Q_s, Q_i)/Q_p$) [2] are shown. A lower Q ratio can yield a larger pair generation rate, however, increasing the Q ratio will asymptotically increase the generated photon state purity γ to a maximum possible value of 1 [2].

An SEM image in Fig. 2(b) shows a subdevice fabricated to test the behavior of the Mach-Zehnder coupler independent of the auxiliary ring. We also fabricated a device with the main ring replaced with a bus waveguide, to characterize the two-point power coupling. Setting $r_{p,e} = r_o$, and setting the signal (and idler) loss rate to $r_e = 2r_o$, we maximize generation rate via equation 1 to demonstrate the concept. Due to fabrication error, we thermally tune to symmetric coupling, as shown in Fig 2(c). Both devices were designed for $r_{p,e} = r_o$. In this custom e-beam process, fabrication resulted in undercoupling of all resonances, which must be recentered for the process to optimize the device. The improvement in η_{FWM} is shown in Fig 2(d), and shows a 3.9 dB increase vs. the equally coupled case without dispersion matching. The passive spectra (no seed lasers or FWM) shown at the top of Fig 2(d), which are normalized to the maximum power, correspond to the right curve in Fig 2(c). A critically coupled pump with half the power coupling as the signal/idler corresponds to ($Q_{s,i}/Q_p$) = 2/3 (measured: $Q_{s,i} = 53k, Q_p = 80k$), η_{escape} = 2/3, or the max value of Fig 2(a).

In this work, we have proposed, and demonstrated subcomponents of, a device capable of generically traversing the γ-η_{escape}-$I_{src,pairs}$ parameter space, while maximizing η_{FWM} by optimizing the main ring cavity geometry and correcting for waveguide and material dispersion via mode splitting with a tunable auxiliary ring. High escape efficiency and purity are crucial from a linear optical quantum computer system design perspective. Future work will characterize the full device, in which we expect a seamless combination of the demonstrated subdevices. Following this we will demonstrate the quantum properties of the device via single photon detection and joint spectral intensity experiments.

Acknowledgments: This work funded in part by Packard Fellowship #2012-38222. Thanks to B. Zhang and D. Gluhovic for insightful feedback.

References

1. T. Rudolph , "Why I am optimistic about the silicon-photonic route to quantum computing", APL Photonics 2, 030901 (2017)
2. Z. Vernon et al., "Truly unentangled photon pairs without spectral filtering," Opt. Lett. 42, 3638-3641 (2017)
3. C. M. Gentry et al., "Tunable coupled-mode dispersion compensation and its application to ... four-wave mixing," Opt. Lett. 39, 5689-5692 (2014)
4. X. Zeng and M A. Popović, "Design of triply-resonant ... parametric oscillators based on Kerr nonlinearity," Opt. Express 22, 15837-15867 (2014)
5. C. M. Gentry, et al., "Tailoring of Individual Photon Lifetimes ... in Quantum Photonic Sources," in CLEO 2016, paper JTu5A.17.